

Length-scale Specific Crystalline Structural Changes Induced by Molecular Randomization of Pequi Oil

Andréa Madalena Maciel Guedes^{1*}, Rosemar Antoniassi¹, Melicia Cintia Galdeano¹, Renato Grimaldi², Mario Geraldo de Carvalho³, Allan Eduardo Wilhelm¹ and Alejandro Gregorio Marangoni⁴

¹ Embrapa Agroindústria de Alimentos, Avenida das Américas, 29501, Guaratiba, 23020-470, Rio de Janeiro, RJ, BRAZIL

² University of Campinas, Rua Bertrand Russel, s/n, Cidade Universitária "Zeferino Vaz" 13083-970 Campinas, SP, Caixa 6091, BRAZIL

³ Rural University of Rio de Janeiro, BR 465, Km. 7, Centro - Seropédica, RJ 23890-000, BRAZIL

⁴ University of Guelph, Guelph, ON, N1G 2W1, CANADA

Abstract: Pequi fruit (*Caryocar brasiliense* Camb) is considered important since its pulp has a high content of oil and carotenoids. The oil's triacylglycerols (TAGs) contain mainly oleic (~57%) and palmitic (~36%) fatty acids, distributed primarily among POO, POP/PPO, and OOO TAGs. It displays a tendency to fractionate upon storage and has a relatively low melting temperature (SFC of 4% at 25°C). Pequi oil was modified through chemical interesterification, which increased the PPP content to ~6%. This caused a flattening in the SFC-temperature profile, raising the end of melt temperature significantly (SFC of 4% at 39°C). The interesterified oil does not fractionate and is thermally stable up to 40°C, with an SFC-temperature profile resembling that of roll-in shortening (SFC of 31% at 16°C) despite containing high amounts of oleic acid. Crystallization and melting behavior changed. Crystal packing became more disorganized as evidenced by a significant decrease in crystalline domain size in the [001] direction from 42.3 nm to 32.1 nm. Polymorphism remained of the triclinic (β) subcell type but polytypism changed from the 3L to the 2L type. Polarized light microscopy demonstrated that interesterification dramatically decreased crystal size, consistent with a higher rate of nucleation in the material. Moreover, the dramatic improvement in physical stability and functionality was not accompanied by a significant decrease in total carotenoid content (~390 mg/kg).

Key words: *Caryocar brasiliense*, interesterification, crystallization, melting, triacylglycerol, crystalline domain size

1 INTRODUCTION

Pequi (*Caryocar brasiliense* Camb) is a native species of fruit from Brazil, found in the Amazon, Caatinga, Cerrado and Atlantic Forest which can offer development opportunities for these regions. Its production of fruit is seasonal, occurring mainly between September and February, with an estimated average production of 7027 ton of fruits in 2011 corresponding to *C. brasiliense* together with *C. coriaceum*¹. In Brazil, pequi is known for its culinary and therapeutic applications.

The fruit is rich in oil (pulp with 36-66% oil d.b.²) with a high content of carotenoids³ and minerals⁴. The oil of pequi pulp contains close to 60% oleic acid (C18:1), a very useful monounsaturated fatty acid for food, cosmetic and oleochemical use due to its high oxidative stability. Pequi oil also contains about 35% palmitic acid (C16:0), which

makes it suitable for margarine and shortening applications.

As a general rule, fats which contain a high proportion of saturated fatty acids are solid at room temperature whereas those in which unsaturated fatty acids predominate, are liquid. Furthermore, the distribution pattern of the fatty acids within TAG molecules is equally important. Additionally, fatty acid chain length, the number and distribution of double bonds, as well as their geometric isomerism (*cis* or *trans*), also strongly influence physical properties⁵.

Natural oils and fats have specific physicochemical properties and very often it is necessary to change these properties, such as melting point and crystallization behavior, in order to achieve specific functionalities for certain applications. One of the most common methods to change physi-

*Correspondence to: Andréa Madalena Maciel Guedes, Embrapa Agroindústria de Alimentos, Avenida das Américas, 29501, Guaratiba, 23020-470, Rio de Janeiro, RJ, BRAZIL

E-mail: andrea.guedes@embrapa.br

Accepted January 17, 2017 (received for review September 29, 2016)

Journal of Oleo Science ISSN 1345-8957 print / ISSN 1347-3352 online

<http://www.jstage.jst.go.jp/browse/jos/> <http://mc.manuscriptcentral.com/jjocs>

cal properties of oils is chemical interesterification, whose redistribution of fatty acids generates a new triacylglycerol (TAG) profile.

In addition, this process does not produce trans fatty acids (TFA), unlike partial hydrogenation. The negative effects of trans fatty acids are well documented⁶⁾ and their specific concentration in foods must be declared by law in some countries. This has led to the loss of GRAS status for partially hydrogenated oils (PHOs) in the United States⁷⁾.

Several studies have utilized chemical interesterification in order to obtain fats with specific physicochemical properties⁸⁻¹⁰⁾. However, chemical interesterification of pequi oil has not been reported.

This work aimed to study the chemical composition, the positional distribution of fatty acids, the crystallization and melting profiles, the solid fat content – temperature profile, the microstructure as well as the polymorphism of pequi oil modified by chemical interesterification to increase its range of plasticity without producing TFA.

2 EXPERIMENTAL

2.1 Raw material

Unrefined artisanal pequi pulp oil was provided by Fazenda Lagoa (Minas Gerais, Brazil).

2.2 Chemical interesterification

Laboratory-scale chemical interesterification was conducted using 100 g of neutralized and dried pequi oil. The reaction was carried out under vacuum with magnetic stirring, with 0.4 % (w/w) sodium methoxide (powder, 95 % purity, Sigma-Aldrich) as catalyzer, during 20 min, at 100°C, according optimization performed by Grimaldi *et al.*¹¹⁾. The reaction was stopped by addition of a 5 % citric acid solution. Soaps were removed by water washing. The product was vacuum dried and stored frozen until analyzed.

2.3 Moisture

The analysis was performed according to Karl-Fischer method using a Karl Fischer Metrohm Titrino plus 870 (Methohm), expressed as mean value (\pm SD) obtained with triplicate samples.

2.4 Peroxide value

The analysis was performed according to AOCS Cd 8b-90 method¹²⁾, with results expressed as mean value (\pm SD) for triplicates.

2.5 Free fatty acids

The analysis was performed according to AOCS Ca 5a-40 method¹²⁾ with results expressed as mean value (\pm SD) for triplicates.

2.6 Carotenoid content

The analysis was carried out by spectrophotometric method using an Agilent 8453 UV-visible spectrophotometer at 450 nm. Spectrophotometric grade hexane was used as solvent. Total carotenoid content was calculated for extinction coefficient (\pm 1 %) of 2500, according to Davies¹³⁾. Briefly, 0.02 g mass was accurately weighted in a 10 mL volumetric flask and the final volume was completed with the organic solvent, in duplicate. A sample portion was transferred to cuvettes and the absorbance was determined. Total carotenoids were calculated as follows:

$$\text{Total carotenoid content (mg/kg)} = \frac{\text{Absorbance} \times 104 \times \text{flask volume (mL)}}{\epsilon_{1\%}^{1\text{cm}} \times \text{weight of oil (g)}}$$

expressed as mean value (\pm SD) obtained with triplicate samples.

2.7 Fatty acid composition

Methyl esters were prepared according to Hartman and Lago¹⁴⁾ method and analyzed by gas chromatography (GC) using an Agilent 7890 chromatographer, equipped with flame ionization detector (FID) set at 280°C. A fused silica capillary column coated with a cyanopropyl syloxane film (60 m \times 0.32 mm \times 0.25 mm) was used. Temperature programming rate: initial temperature: 100°C for 3 min; 50°C/min to 150°C; 1°C/min to 180°C; 25°C/min to 200°C; final temperature: 200°C for 10 min. 1 μ L of 2 % solution diluted in dichloromethane was injected in an injector heated to 250°C working at 1:50 flow division mode. The identification was made by comparison of retention times of Nu-Chek-Prep Inc. (Elysian, MN) standards and the quantification was performed by internal normalization, with results expressed as mean value (\pm SD) obtained with triplicate samples.

2.8 Iodine index and saponification value

Iodine index and saponification value were calculated from the fatty acid composition run in triplicate according to AOCS Cd 1c-85 and AOCS Cd 3a-94 methods, respectively¹²⁾.

2.9 Triacylglycerol composition

High performance liquid chromatography analysis was carried out using a Waters Alliance model 2690 (Milford, USA) chromatographer equipped with vacuum degasser, auto sampler, temperature-controlled column oven and a refractive index (RI) detector Waters model 2410. For the TAG separation, a Waters XBridgeTM C18 column (5 μ m, 4.6 \times 250 mm) was used. The analytes were eluted after injecting 10 μ L of sample, using an isocratic solvent system consisting of 60/40 % v/v acetone/acetonitrile. The flow rate was maintained at 1 mL/min. The separation time was 40 minutes. During analysis, the sample chamber, column oven and RI detector were kept at 40°C. Results were expressed as mean value (\pm SD) obtained with triplicate

samples.

2.10 Positional distribution of fatty acids

The NMR spectra were recorded on a Bruker Advance II 400 MHz spectrometer operating at 400 MHz for proton and 100 MHz for ^{13}C . ^{13}C -NMR spectra were used to analyze the positional distribution of fatty acids on the glycerol backbone. Oil samples (10 mg) were dissolved in CDCl_3 (deuterated chloroform) (1.0 mL), with TMS (tetramethylsilane) as reference, in 5 mm NMR tubes and experiments were conducted at 25°C . The ^{13}C spectra of the lipid samples were acquired with a spectral width of 65535 Hz, pulse of 9.13 ms, and a relaxation delay of 2.0 s with Dep-tqgpcsp pulse program. Carboxyl signals allowed determining the *sn*-1,3 and *sn*-2 position of saturated and unsaturated fatty acids. The spectra were processed using the ACD/NMR Processor Academic Edition Program (Version 12.0).

2.11 Solid Fat Content - SFC

The analysis was performed by pulsed Nuclear Magnetic Resonance spectroscopy (p-NMR) using a Bruker MQ20 pulsed NMR analyzer, according to the AOCS method Cd 16b-93¹²⁾ at 10, 20, 25, and 30°C for the original samples and at 10, 20, 25, 30, 35, 40, and 45°C for chemically interesterified samples.

2.12 Melting point

The melting temperature was determined from the temperature corresponding to 4% solids from the SFC-temperature profile¹⁵⁾. In addition, the slip melting point was determined using the AOCS Cc 3-25 open capillary method¹²⁾, in triplicate.

2.13 Thermal analysis

The DSC (Differential Scanning Calorimetry) curves were obtained using a Q200 DSC (TA Instruments, New Castle, USA) according to AOCS Cj 1-94 method¹²⁾. Samples of 5-6 mg weight were placed in sealed aluminum pans and analyzed for both crystallization and melting behavior under a cooling rate of $-5^\circ\text{C}/\text{min}$ ranging from 80°C to -70°C with an isothermal time of 10 min at 80°C to erase thermal history, and a heating rate of $5^\circ\text{C}/\text{min}$ ranging from -70°C to 80°C with an isothermal time of 30 min at -70°C . An empty aluminum pan was used as reference. The curves were analyzed for the onset of crystallization (T_{pc} , $^\circ\text{C}$), peak crystallization (T_{pc} , $^\circ\text{C}$) and final crystallization (T_{fc} , $^\circ\text{C}$) temperatures, crystallization enthalpies (ΔH_c , J/g), onset of melting (T_{om} , $^\circ\text{C}$), peak melting (T_{pm} , $^\circ\text{C}$) and final melting (T_{fm} , $^\circ\text{C}$) temperatures, as well as melting enthalpies (ΔH_m , J/g), expressed as mean value (\pm SD) obtained with triplicate samples. Calibration was carried out with indium standard (m.p. 156.5°C , ΔH 28.45 J/g).

2.14 Light microscopy analysis

A drop of molten pequi oil was placed on a microscope slide at 80°C and a 80°C heated coverslip was placed on top. The sample was then cooled statically to 20°C . Polarized light microscopy (PLM) images were obtained using an Olympus Model BX60 F5 light microscope (Olympus Optical Co. Ltd., Tokyo, Japan). The CellSens Entry software (Olympus Canada Inc., Toronto, Canada) was used to obtain digital photos of fat crystals. Micrographs were enhanced using Photoshop CS1 (Adobe Systems, San Jose, CA, USA).

2.15 Polymorphism

Approximately 1 g of each sample was placed onto an Aluminum sample holder with a depth of 2 mm, which itself was placed on top of a home-made cooling platform. The platform allows water to circulate inside it which in turn maintains a fixed temperature on the sample holder. The sample temperature was monitored directly and equilibrated to room temperature (20°C) prior to polymorphism characterization by powder X-ray diffraction (XRD) using a Rigaku Multiflex powder X-ray diffraction unit (Rigaku, Tokyo, Japan). The copper lamp (Cu $K\alpha_1$) was operated at 40 kV and 44 mA with the use of the following slits: divergence (0.5°), scatter (0.5°) and receiving (0.3°). For both small-angle X-ray diffraction analysis (SAXD) and wide angle X-ray diffraction (WAXD), samples were scanned from 0.5 to 30° at $0.02^\circ/\text{min}$. MDI Jade 6.5 software (Rigaku, Tokyo, Japan) was used to analyze the acquired patterns in both WAXD and SAXD and define peak positions. Polymorphic forms were identified from the WAXD region of 2θ : 13 - 30° , as described by Larsson¹⁶⁾.

The crystalline domain size of TAG crystalline nanoplatelets (CNP) can be determined from SAXD measurements of diffraction peak width, using the Scherrer equation¹⁷⁾, $D = K\lambda/\text{FWHM} \cos(\theta)$, where: K , the Scherrer constant or the shape factor, was taken as 0.9; λ : 1.54 \AA , (the X-ray wavelength for the copper anode); FWHM (full width at half maximum, rad) was determined from the first small angle reflection, corresponding to the (001) plane¹⁷⁾; and θ is the Bragg angle [$^\circ$]¹⁷⁾. The Scherrer equation is used to estimate mean crystal domain sizes up to 100 nm and monodisperse crystal distributions are assumed. In order to accurately determine the value of the crystalline domain size, instrument-related factors that influence peak width and shape need to be determined. This was not done in this study and thus the exact value of the domain size could not be obtained. However, the relative changes observed in domain size remain valid and useful.

The X-ray spectra were analyzed using MDI Jade V 9.0.1 (Livermore, California, USA) to obtain the desired parameters from the XRD patterns. Peaks were fitted using either a Gaussian function (WAXS region) or a Pearson VII function (SAXS region). A straight line was used as back-

ground. A deconvolution of the peaks was carried out to minimize the residual error function, R. This is achieved by means of a non-linear least-square fitting routine based on the Levenberg-Marquardt method. The software provides the angle at which the maximum of the fitted Bragg peak appears, the d-value (interplanar separation) associated with that angle and the full width at half maximum (FWHM) of the fitted peak. This allowed for peak asymmetries related to beamstop and slits effects to be eliminated.

3 RESULTS AND DISCUSSION

The oil used as raw material contained 0.07% moisture, apart from a low free fatty acids content and peroxide value (Table 1). Low levels are prerequisites for carrying

out interesterification using a chemical catalyst⁴⁾. After interesterification, washing and drying of the oil, moisture remained unaltered while a significant increase in acidity occurred which is expected after interesterification due to hydrolysis with consequent increase in partial glycerides. On the other hand, no increase in the peroxide value was observed, suggesting this process did not promote oil oxidation.

Carotenoid content in the oil did not decrease significantly ($p > 0.05$) after interesterification (from 398.2 mg/kg to 382.5 mg/kg) and both contents were close to the range reported by other authors³⁾.

The fatty acid profile of the samples (Table 2) is similar to that reported by Facioli and Gonçalves¹⁷⁾ and Faria-Machado *et al.*²⁾. The content of C18:2 and C18:3 were 2 and 0.3%, respectively, explaining the good oxidative sta-

Table 1 Characterization of non-interesterified and interesterified pequi oil.

	Moisture (%)	Free fatty acids (%)*	Peroxide value (meq/kg)	Carotenoid content (mg/kg)
A	0.07 ± 0.00 ^a	0.52 ± 0.02 ^a	0.60 ± 0.11 ^a	398.2 ± 8.55 ^a
B	0.07 ± 0.00 ^a	1.18 ± 0.04 ^b	0.41 ± 0.11 ^b	382.5 ± 7.64 ^a

A: non-interesterified pequi oil; B: interesterified pequi oil. Same letters in the same column are not significantly different from each other (Tukey test, $p > 0.05$). * Expressed as oleic acid.

Table 2 Fatty acid composition, iodine value and saponification value of non-interesterified and interesterified pequi oil.

Fatty acid	Oil (%)		
	A	B	C*
La (C12:0)	tr.	tr.	n.d.
M (C14:0)	tr.	tr.	n.d.
P (C16:0)	35.78 ± 0.39 ^a	35.84 ± 0.26 ^a	40.2
Po (C16:1)	1.03 ± 0.04 ^a	1.02 ± 0.04 ^a	1.4
St (C18:0)	2.20 ± 0.05 ^a	2.21 ± 0.03 ^a	2.3
O (C18:1)	57.52 ± 0.44 ^a	56.93 ± 0.23 ^a	53.9
L (C18:2)	1.99 ± 0.07 ^a	2.02 ± 0.15 ^a	1.5
Ln (C18:3)	0.33 ± 0.01 ^a	0.32 ± 0.01 ^a	0.7
Ar (C20:0)	tr.	tr.	0.2
G (C20:1)	0.24 ± 0.01 ^a	0.24 ± 0.00 ^a	n.d.
Iodine value	55.05	55.76	—
Saponification value	197.49	197.60	—

A: non-interesterified pequi oil; B: interesterified pequi oil; C*: non-interesterified pequi oil – data obtained by Facioli and Gonçalves¹⁷⁾; La: lauric acid; M: myristic acid; P: palmitic acid; Po: palmitoleic acid; St: stearic acid; O: oleic acid; L: linoleic acid; Ln: linolenic acid; Ar: arachidic acid; G: gadoleic acid; tr.: traces. n.d. non-detected. Same letters in the same line are not significantly different from each other (Tukey test, $p > 0.05$).

bility of the oil. The same fatty acid composition was observed in the interesterified oil, since interesterification does not lead to changes in fatty acid profile, and, as expected, the reaction did not affect the iodine value of the studied oil⁵⁾.

Melting point measured by open capillary method was 25.7°C in the raw material and 41.6°C in the interesterified sample. This higher melting point may allow the interesterified oil to provide structure to the products containing them, besides enabling its use in the production of margarines and shortening, among others. The change in melting point is indicative that new TAG molecular species had been created, including possibly creation of disaturated (S_2U) and trisaturated (S_3) TAGs where S stands for saturated fatty acid (S) and U stands for unsaturated fatty acid (U). This would have also lead to an increase in the plastic range of the fat.

The TAGs present in pequi oil are predominantly POP, POO and OOO (Table 3). The level of POST differed from that found by Facioli and Gonçalves¹⁹⁾, being approximately 65% lower in the current study. Variations in TAG composition may occur among samples of the same species collected from different geographic locations and during different growing seasons. POP, a TAG of great importance for chocolate industry, was 34% in non-interesterified pequi oil. Cocoa butter is the main component in chocolate whose major TAGs are POP, POST and StOSt. Cocoa butter equivalents or extenders, such as palm mid fraction, have been studied based on their TAG composition similarities and compatibility²⁰⁾.

Reduction of the S_2U content (POP + POS) from 37 to 25% in the present study and the consequent reduction in the steepness of the SFC curve may also be explained from changes in TAG composition. Other changes observed were an increase in the content of PPP and OOO. Increases in S3 and decreases in S_2U contribute to the structure and lubricity of the resulting fat²¹⁾.

The stereospecific distribution of fatty acids within TAG molecules can be identified by the chemical shift of carboxyl carbons. The expansion and integration of signals in the ^{13}C -NMR spectrum in the frequency region of carboxyl groups of the original oil (A) as well as of the interesterified product (B) makes it possible to observe the transfer of acyl

groups in the TAG structure through the resulting randomization of the fatty acids.

From the ^{13}C -NMR spectrum of the non-interesterified oil it was possible to infer that 61.5% of all fatty acids at positions *sn*-1 and *sn*-3 were saturated (δ 173.1190 ppm), and 38.5% unsaturated (δ 173.0937 ppm). There was only one signal at the chemical shift region for carboxyl groups in *sn*-2 position, corresponding to that of unsaturated fatty acids (δ 172.6956 ppm)²²⁾. The ^{13}C -NMR spectrum of the interesterified oil displayed two signals in the *sn*-2 region, with 42% corresponding to saturated fatty acids. This shows that after chemical interesterification there is a more random distribution of saturated and unsaturated fatty acids within the TAG structures. ^{13}C -NMR of tripalmitin (PPP, S3) (Fig. 1) confirms the chemical shift for saturated fatty acids in the regions of δ 173 ppm and δ 172 ppm for position *sn*-1,3 and *sn*-2, respectively.

The measurement of solid fat content (SFC) as a function of temperature has been widely used to determine the structural-functional properties of fats, where molecular composition is regarded as the main factor affecting this SFC²³⁾. Interesterification reduced the steepness of the SFC-T curve showing decreased SFC from 20 to 45°C, thus increasing its plastic range (Fig. 2). An increase in SFC at higher temperatures was mainly due to increase in PPP/PPS.

Changes in SFC resulting from interesterification can lead to an increase in the plastic range of the fat. This is quite important since native pequi oil has very limited functionality as a food product. An SFC of 68% at 10°C suggests an extremely hard and brittle fat, which rapidly melts displaying an SFC of 4% at 25°C and a complete melt by 30°C, well below body temperature and in the range of room temperature in many households. A margarine or shortening made with native pequi oil would be almost liquid at 25°C. This profile is far from being ideal. Interesterified pequi oil, on the other hand, has an SFC of 45% at 10°C, making it much softer material at this temperature, and an SFC of 5% at 40°C, suggesting its possible use as heat-resistant spread²⁴⁾. Overall, interesterified pequi oil SFC-T resembles traditional roll-in shortenings, in which SFC ranges from 40 to 10% at 10 to 33.3°C²¹⁾, e.g., SFC of 31% at 16°C.

Table 3 Triacylglycerol composition of non-interesterified and interesterified pequi oil.

Oil	TAG (%)									
	OOL	POL	PPL	OOO	POO	POP	PPP	StOO	POST	PPSt
A	1.1 ± 0.1	2.2 ± 0.1	0.6 ± 0.1	10.5 ± 0.1	38.7 ± 0.6	33.7 ± 0.8	0.3 ± 0.1	2.1 ± 0.1	3.2 ± 0.1	nd.
B	1.6 ± 0.1	2.2 ± 0.1	0.6 ± 0.1	15.7 ± 0.1	32.9 ± 0.1	22.8 ± 0.1	5.2 ± 0.1	1.7 ± 0.1	2.4 ± 0.0	0.7 ± 0.1

A: non-interesterified pequi oil; B: interesterified pequi oil; O: oleic acid; P: palmitic acid; L: linoleic acid; St: stearic acid; n.d.: not detected.

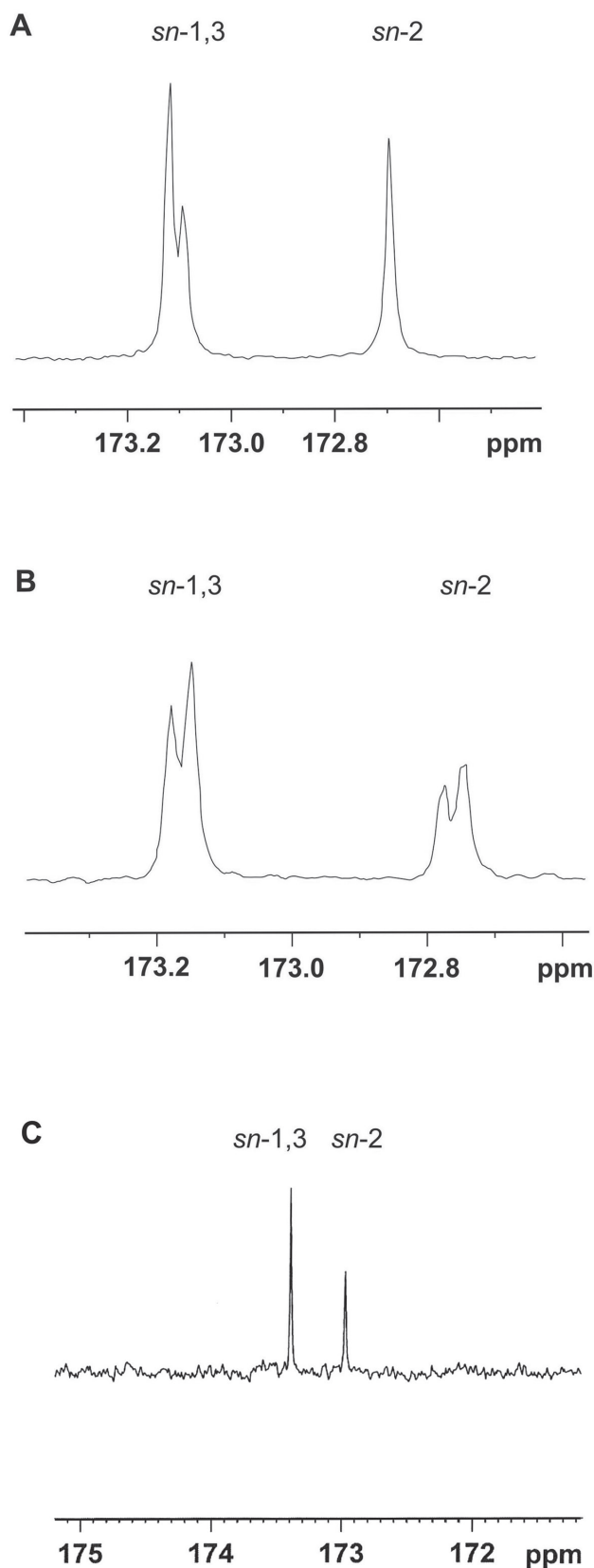


Fig. 1 ^{13}C -NMR spectra of non-interesterified (a), interesterified pequi oil (b) and tripalmitin (c).

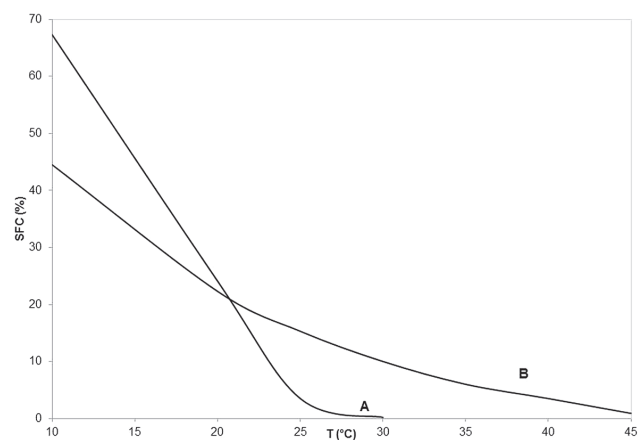


Fig. 2 Solid fat content (SFC) vs. temperature of oil non-interesterified (a), interesterified (b) pequi oil.

The temperature at which an SFC of 4% is observed has been correlated to the melting point of a fat¹⁵⁾. For non-interesterified and interesterified pequi oil, the melting point obtained by this method was 24.7°C and 38.9°C, respectively.

Thermal events observed by DSC curves may suggest the presence of distinct TAG fractions in the oil. In the crystallization curves shown in Fig. 3, an additional peak can be found for interesterified pequi oil (B) at higher temperatures. This peak may correspond to a higher melting fraction composed of PPP and PPSt, formed during interesterification.

The melting curves also show different behavior between samples (Fig. 4), with a higher final melting temperature (T_{fm}) for the interesterified oil. The major changes were observed in the middle-melting peaks region corresponding to POP-PPO, whose content diminished upon interesterification. This translated to the broadening of the melting peak in the characteristic melting region for β form of POP

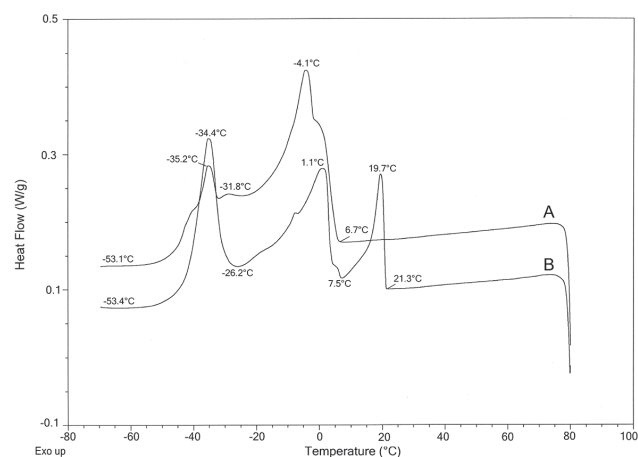


Fig. 3 DSC crystallization curves of non-interesterified (a), interesterified (b) pequi oil.

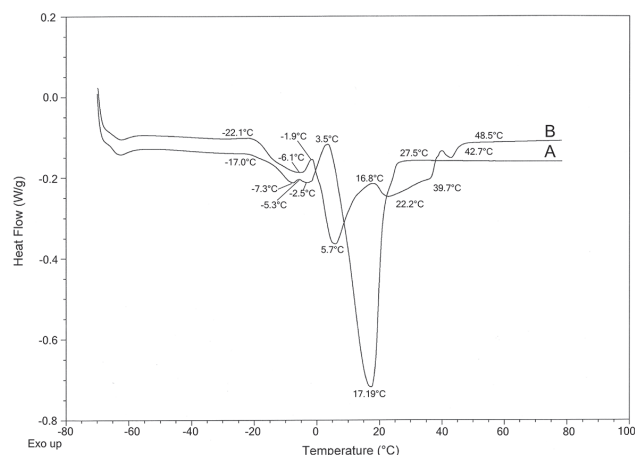


Fig. 4 DSC melting curves of non-interesterified (a), interesterified (b) pequi oil.

from 17 to 39°C (m.p. $\sim 35^{\circ}\text{C}$)²⁵⁾. Interestingly, the melting profile also reveals a broadening of the melting peak of the β form of OOO, around 5°C ²⁶⁾ upon interesterification. All these changes in thermal events upon interesterification took place while maintaining a similar melting enthalpy ($\Delta H_B = 78.24 \text{ J/g}$) when compared to the original oil ($\Delta H_A = 71.48 \text{ J/g}$). Finally, compared to non-interesterified pequi oil, the interesterified pequi oil melting profile displayed wider and less defined peaks, as well as a wider melting temperature range and final melting temperature, reflecting the changes observed in the SFC-T curves and TAG composition.

Fat crystal networks can be observed in the length scales of 1–200 μm , the mesoscale, under polarized light microscopy. A great change in the crystal morphology of pequi oil took place upon interesterification (Fig. 5). Prior to interesterification, pequi oil displayed spherulite-shaped crystals with considerable space between adjacent crystals. The crystals in non-interesterified pequi oil were large and coarse, and crystals of approximately 100 μm in length were found in the samples even without aging. These crystals can be responsible for grainy appearance in shortenings, fractionation and separation of oil, and are suggestive of a non-functional fat for many industrial applications. For interesterified oil, smaller crystal sizes were observed, suggestive of enhanced nucleation and a more rapid crystallization process.

The polymorphism of the crystallized non-interesterified and interesterified pequi oil was analyzed by powder X-ray diffraction (XRD), where the lateral and longitudinal packing, and stacking, of fatty acid chains are identified from the short- and long-spacings, respectively. Compared to pure compounds, diffraction patterns of natural fats produce broader peaks, as they contain a wide range of fatty acids groups²⁷⁾. The typical strong diffraction peak corresponding to a short-spacing (wide angle of 4.6 \AA) of β -form was present in both non-interesterified and inter-

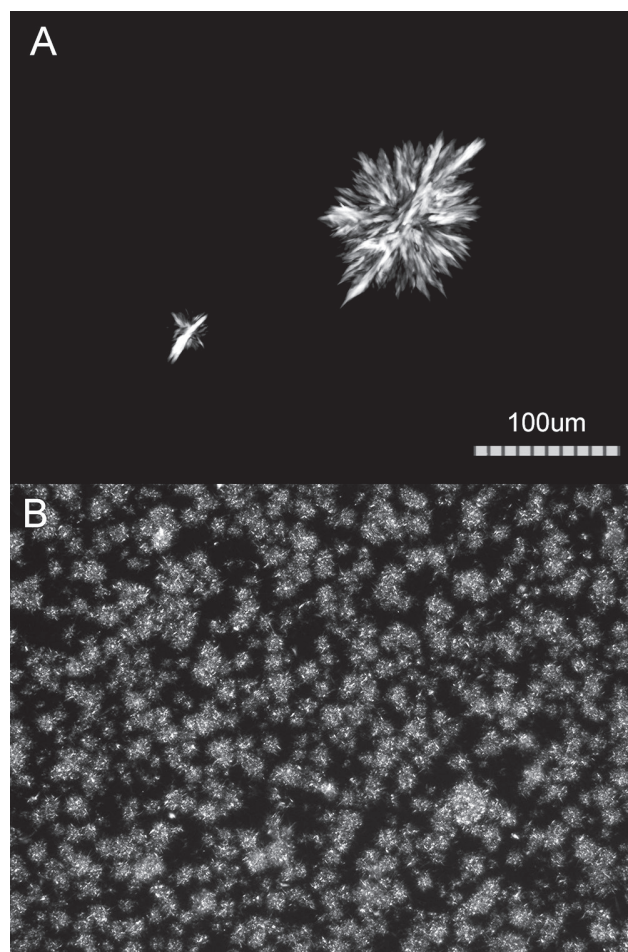


Fig. 5 Polarized light micrographs obtained by static crystallization of non-interesterified (a), interesterified (b) pequi oil at 20°C .

esterified pequi oil (Fig. 6C, D).

Since the β polymorphic form of TAGs is the thermodynamically most stable crystal form, both non-interesterified and interesterified pequi oil will not recrystallize upon storage or temperature fluctuations. This translates to a greater physical stability of the fat. This is in contrast to many industrial fats where the polymorphic transition from β' to β is likely to take place upon storage or temperature abuse, such as palm oil²⁴⁾. Moreover, fats in the β -form have been recently shown to be suitable for use as roll-in shortening²⁸⁾.

Different crystal sizes and shapes can be obtained for the same polymorphic form, influencing the graininess and rheological properties of the product⁸⁾. In other words, the same polymorph found in crystal aggregates of certain fat products, such as margarine or shortening, may have different microstructures²⁴⁾, as it was seen in non-interesterified and interesterified pequi oil, representing modifications induced by structural rearrangements at the nanoscale.

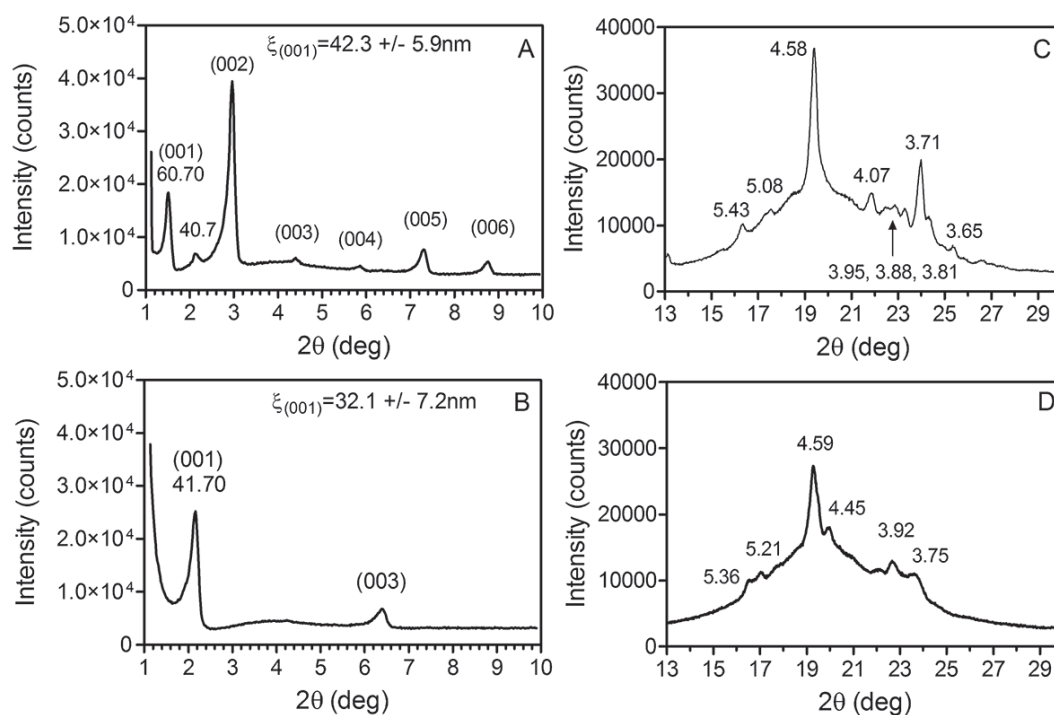


Fig. 6 Representative powder WAXS and SAXS diffraction spectra for non-interesterified (a), interesterified (b) pequi oil at 20°C. The domain size reported in the SAXS region represents the average width and standard deviation of $n=6$ (non-interesterified) and $n=4$ (interesterified) peaks.

Triple chain length (3L) packing of non-interesterified pequi oil changed to double chain (2L) stacking upon interesterification. Mono-acid TAGs polymorphs tend to crystallize in 2L polytypes, while the β -form of the symmetrical unsaturated (SUS) TAGs, such as POP and SOS, tends to pack in the 3L form²⁵⁾. The overall change in the lamellar stacking of TAGs in pequi oil upon interesterification seems to be influenced by the increase in PPP and PPSt and a reduction in the POP content.

A crystal domain size of 42.3 nm for non-interesterified (A) and 32.1 nm for interesterified (B) pequi oil was determined from the reflections arising from the (001), (002) and (003) planes as indicated in **Fig. 6**. This decrease was statistically significant ($p < 0.05$, $n = 6$, $n = 4$, for non-interesterified and interesterified oil, respectively). Even though the intersolubility of TAGs resulting from the formation of new TAGs had not affected the energetic requirement for melting, the rearrangement seems to have induced modifications at the nanoscale leading to a decrease in domain size. Peak width and the corresponding domain size calculated is a function of both the physical dimension of the structure diffracting X-rays and the "order" in the packing of the diffracting planes. In our case, if the stacking of TAG lamellae became disordered, this would translate to a decrease in domain size as well. This does not mean that the physical dimension of the CNP thickness is changing, but that the packing of the molecules is becoming more disordered. The domain size is more properly considered a cor-

relation length or persistence length of the scattering event, rather than a physical dimension. Of course, if a complementary technique is used to confirm the physical dimension of the structure, such as transmission electron microscopy (TEM), then one can confidently state that the domain size corresponds to the thickness of the CNP. An important point that needs to be mentioned here is that the domain size is a strong function of the supersaturation conditions during crystallization^{18, 29)}, namely increases in supersaturation lead to decreases in domain size. Our data suggests that interesterification increased the melting point of the pequi oil by $\sim 14^\circ\text{C}$, judging from the temperature corresponding to an SFC of 4%. This increased supersaturation would lead to a greater surface nucleation of TAGs during crystallization. This more stochastic surface nucleation would lead to a more disordered growth in the [001] direction. Thus, the observed changes in domain size were most probably due to a differential supersaturation effect induced by interesterification.

Furthermore, it is possible that a more disordered crystalline growth at the nanoscale constitutes the reason why large crystalline structures were not formed upon interesterification. Due to nanoscale disordering, crystalline growth at the mesoscale probably became energetically quite expensive, thus favoring nucleation. This increased nucleation was responsible for the smaller crystal size observed by light microscopy. Thus, this constitutes an interesting way of controlling nucleation events by randomiza-

tion of structure at the nanoscale. We are investigating this strategy further.

4 CONCLUSION

Here we show that random interesterification of pequi oil led to the formation of a functional food fat. Native pequi oil lacks the melting behavior and thermo-mechanical properties required for food functionality. Therefore, interesterification of pequi oil will greatly increase the range of applications of this oil, and thus its added value along the entire pequi oil value chain.

ACKNOWLEDGMENTS

The authors are grateful for the financial support provided by the Brazilian research funding agency FAPERJ, and the Natural Sciences and Engineering Research Council of Canada (NSERC).

REFERENCES

- 1) Instituto Brasileiro de Geografia e Estatística (2011) [Internet]. Produção da extração vegetal e da silvicultura. http://www.ibge.gov.br/home/estatistica/economia/pevs/2011/default_xls.shtm. Accessed Dec. 2015.
- 2) Faria-Machado, A.F.; Tres, A.; van Ruth, S.M.; Antoniassi, R.; Junqueira, N.T.V.; Lopes, P.S.N.; Bizzo, H.R. Discrimination of pulp oil and kernel oil from pequi (*Caryocar brasiliense*) by fatty acid methyl esters fingerprinting, using GC-FID and multivariate analysis. *J. Agric. Food Chem.* **63**, 10064-10069 (2015).
- 3) Aquino, L.P.; Ferrua, F.Q.; Borges, S.V.; Antoniassi, R.; Correa, J.L.G.; Cirillo, M.A. Influence of pequi drying (*Caryocar brasiliense* Camb.) on the quality of the oil extracted. Influência da secagem do pequi (*Caryocar brasiliense* Camb.) na qualidade do óleo extraído. *Food Sci. Technol. (Campinas)* **29**, 354-357 (2009).
- 4) Mariano-da-Silva, S.; Brait, J.D.A.; de Faria, F.P.; da Silva, S.M.; de Oliveira, S.L.; Braga, P.F.; Mariano-da-Silva, F.M.S. Chemical characteristics of pequi fruits (*Caryocar brasiliense* Camb.) native of three municipalities in the State of Goiás - Brazil. *Cienc. Tecnol. Aliment* **29**, 771-777 (2009).
- 5) O'Brien, R.D. Fats and Oils Formulation. in *Fats and oils: formulating and processing for applications* (O'Brien, R.D. ed.). CRC Press, Boca Raton (2009).
- 6) Mozaffarian, D.; Katan, M.B.; Ascherio, A.; Stampfer, M.J.; Willett, W.C. Medical progress - Trans fatty acids and cardiovascular disease. *N. Engl. J. Med.* **354**, 1601-1613 (2006).
- 7) Food and Drug Administration. Final determination regarding partially hydrogenated oils (removing trans fat). <http://www.fda.gov/Food/IngredientsPackagingLabeling/FoodAdditivesIngredients/ucm449162.htm>. Accessed February 2016.
- 8) Ahmadi, L.; Marangoni, A.G. Functionality and physical properties of interesterified high oleic shortening structured with stearic acid. *Food Chem.* **117**, 668-673 (2009).
- 9) Guedes, A.M.M.; Ming, C.C.; Ribeiro, A.P.B.; da Silva, R.C.; Gioielli, L.A.; Gonçalves, L.A.G. Physicochemical properties of interesterified blends of fully hydrogenated Crambe abyssinica oil and soybean oil. *J. Am. Oil Chem. Soc.* **91**, 111-123 (2014).
- 10) Soares, F.A.S.M.; Silva, R.C.; Hazzan, M.; Capacla, I.R.; Viccola, E.R.; Maruyama, J.M.; Gioielli, L.A. Chemical interesterification of blends of palm stearin, coconut oil, and canola oil: Physicochemical properties. *J. Agric. Food Chem.* **60**, 1461-1469 (2012).
- 11) Grimaldi, R.; Gonçalves, L.A.G.; Ando, M.Y. Optimization of the chemical interesterification reaction of palm oil. *Quim. Nova* **28**, 633-636 (2005).
- 12) American Oil Chemists' Society. Official methods and recommended practices of the AOCS. AOCS Press, Champaign, IL, USA (2009).
- 13) Davies, B.H. Carotenoids. in *Chemistry and biochemistry of plant pigment* (Goodwin, T.W. ed.). Academic Press, London, pp. 38-165 (1976).
- 14) Hartman, L.; Lago, R.C.A. Rapid preparation of fatty acid methyl esters from lipids. *Lab. Pract.* **22**, 475-476 (1973).
- 15) Karabulut, I.; Turan, S.; Ergin, G. Effects of chemical interesterification on solid fat content and slip melting point of fat/oil blends. *Eur. Food Res. Technol.* **218**, 224-229 (2004).
- 16) Larsson, K. Classification of glyceride crystal forms. *Acta Chem. Scand.* **20**, 2255-2260 (1966).
- 17) West, A.R. (ed.) *Solid state chemistry and its applications*. John Wiley & Sons, West Sussex (1984).
- 18) Acevedo, N.C.; Marangoni, A.G. Toward nanoscale engineering of triacylglycerol crystal networks. *Cryst. Growth Des.* **10**, 3334-3339 (2010).
- 19) Facioli, N.L.; Gonçalves, L.A.G. Piqui (*Caryocar brasiliense* Camb) oil triglyceride composition modification by enzymatic way. *Quim. Nova* **21**, 16-19 (1998).
- 20) Shukla, V.K.S. Confectionary lipids. in *Bailey's industrial oil and fat products* (Shahidi, F. ed.). John Wiley & Sons, New Jersey (2005).
- 21) Macias-Rodriguez, B.; Marangoni, A.G. Physicochemical and rheological characterization of roll-in shortenings. *J. Am. Oil Chem. Soc.* **93**, 575-585 (2016).
- 22) Ng, S. Quantitative analysis of partial acylglycerols and free fatty acids in palm oil by C-13 nuclear magnetic

- resonance spectroscopy. *J. Am. Oil Chem. Soc.* **77**, 749-755. (2000).
- 23) Rye, F.F.; Litwinenko, J.W.; Marangoni, A.G. Fat crystal networks. in *Bailey's industrial oil and fat products* (Shahidi, F. ed.). John Wiley & Sons, New Jersey (2005).
- 24) Ghotra, B.S.; Dyal, S.D.; Narine, S.S. Lipid shortenings: a review. *Food Res. Int.* **35**, 1015-1048 (2002).
- 25) Sato, K.; Arishima, T.; Wang, Z.H.; Ojima, K.; Sagi, N.; Mori, H. Polymorphism of POO and SOS. I. Occurrence and polymorphic transformation. *J. Am. Oil Chem. Soc.* **66**, 664-674 (1989).
- 26) Sato, K.; Ueno, S. Polymorphism of fats and oils. in *Bailey's industrial oil and fat products* (Shahidi, F. ed.). Wiley & sons, New Jersey (2005).
- 27) Rousseau, D.; Marangoni, A.G.; Jeffrey, K.R. The influence of chemical interesterification on the physico-chemical properties of complex fat systems. 2. Morphology and polymorphism. *J. Am. Oil Chem. Soc.* **75**, 1833-1839 (1998).
- 28) Acevedo, N.C.; Marangoni, A.G. *U.S. Pat.* 14122846 (2012).
- 29) Acevedo, N.C.; Marangoni, A.G. Characterization of the nanoscale in triacylglycerol crystal networks. *Cryst. Growth Des.* **10**, 3327-3333 (2010).
-